International Journal of Medical, Medicine and Health Sciences
ISSN: 2517-9969
Vol:5, No:9, 2011

Bleeding Detection Algorithm for Capsule Endoscopy

Yong-Gyu Lee and Gilwon Yoon*

***Abstract*—**Automatic detection of bleeding is of practical importance since capsule endoscopy produces an extremely large number of images. Algorithm development of bleeding detection in the digestive tract is difficult due to different contrasts among the images, food dregs, secretion and others. In this study, were assigned weighting factors derived from the independent features of the contrast and brightness between bleeding and normality. Spectral analysis based on weighting factors was fast and accurate. Results were a sensitivity of 87% and a specificity of 90% when the accuracy was determined for each pixel out of 42 endoscope images.

***Keywords*—**bleeding, capsule endoscopy, image analysis, weighted spectrum

I. Introduction

WIRELESS capsule endoscopy (WCE) has an advantage of examining all the digestive tract unlike gastrointestinal endoscopy, push enteroscopy and enteroclysis [1-3]. Once a patient swallows a small capsule, it travels in the digestive tract and sends the images to the data receiver wirelessly. WCE has an additional merit of measuring the endoscopic images during daily activities. As an example in case of [3], WCE is composed of a light source, often LED, collecting lens, an image sensor such as CMOS or CCD, transmitter, antenna and battery as illustrated in Fig. 1. The capsule travels from the mouth to the large intestine propelled by peristalsis and digestive fluid. Each image has a resolution of 320 x 320 with a speed of three frames/second or images/second. An 8-hour recording produces about 86,400 images to be examined. A specialist faces a task of handling such an enormous amount of the images and finding out the abnormality somewhere in thousands of the images. Therefore, a supportive diagnostic program can be very helpful. Bleeding is one of the salient abnormal conditions. Blood is also associated with other diseases such as vascular rupture, tumor, ulcer, Crohn's disease and angiodysplasia [4-5]. Because of these reasons, bleeding detection is a very good candidate for automatic diagnosis.

However, bleeding does not show a certain unique pattern or distribution. It dose not appear to be straightforward to detect bleeding because there are many complications involved. For example, blood shows different red colors depending on the oxygenation level. We see further different shades from blood when it is mixed with secreted fluid or food dregs. We do not have always a uniform illumination light. The camera angle is not always the same. Detector sensitivity with respect to wavelength may vary. Due to all these circumstances, we should have color compensations in any manner. To solve these problems, this study proposes a bleeding detection algorithm that gives weighting factors on key spectra. This is based on the contrasting features between blood and normal tissues. And experimental verifications were followed.

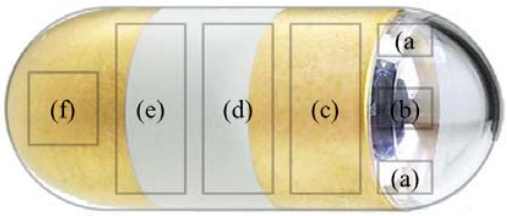

Fig.1 An example of capsule configuration; (a) LEDs, (b) lens, (c) image array sensor, (d) battery, (e) transmitter, (f) antenna.

II. Methodology

A. Overall Architecture

Our proposed algorithm has a total of six steps. They are Input Movies, Preprocessing, Feature Extraction, Analysis & Classification, Verification and Output Movies. This is shown in Fig. 2.

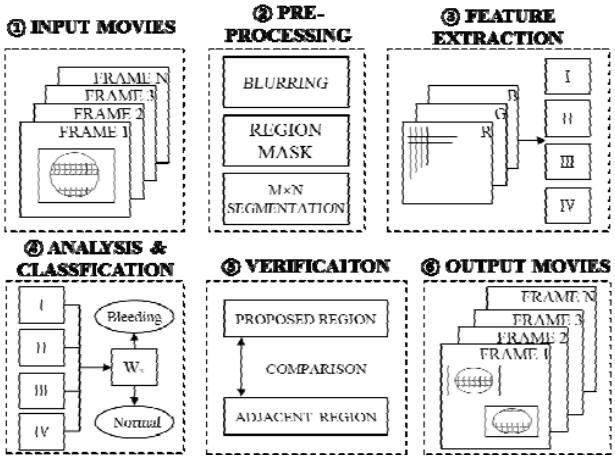

Fig. 2 The overall schematic of the proposed algorithm

In the step of Input Movies, the images (frames) acquired from the capsule are arranged in a row. Computation is done for each frame. The purpose of Preprocessing is to have operations faster and to get reliable image data with reduced noise.

Y-G Lee is with Seoul National University of Science and Technology, Seoul, KOREA (e-mail: yglee@seoultech.ac.kr).
G. Yoon is also with Seoul National University of Science and Technology, Seoul, KOREA (phone: 82-2-970-6419; fax: 82-2-979-7903; e-mail: gyoon@seoultech.ac.kr). *Correspondence to G. Yoon.

Masking, filtering and segmentation are performed. In Feature Extraction, color, saturation and proportions with respect to wavelengths are computed in order to extract the contrasting features between blood and normal tissue. In Analysis & Classification, weighting factors are calculated from the contrasting features and applied to a corresponding frame in order to enhance bleeding region. In this process, potential bleeding regions are selected. In the step of Verification, bleeding regions are finally diagnosed after they are compared to the neighboring regions and pass certain criteria. In Output Movies, all the analyzed frames are rearranged to create the enhanced images of bleeding.

B. Preprocessing

Images are being low-frequency filtered spatially, which reduces noises and produce clean images. Tissue color in the endoscopic image provides with valuable information. For instance, white is caused by too much illumination and black is low illumination. Yellow may be related with pus and information on the digestive organ can be deduced from red [4]. Therefore, we masked the pixels that did not have red color. We also did not use any black region. For red (R), green (G), blue (B) values of the pixel, Eq. (1) masks any color except red. Eq. (2) differentiates pixels from black and white. In our case, we set d_1=0.25, d_2=50 and d_3=490.

$$\max(R_{(i,j)}, G_{(i,j)}, B_{(i,j)}) = R_{(i,j)} \wedge \frac{G_{(i,j)} + B_{(i,j)}}{R_{(i,j)} + \min(G_{(i,j)}, B_{(i,j)})} > d_1 \quad (1)$$

where i, j*: natural number*

$\wedge$ *represents AND logical operation*

$$\sqrt{R_{(i,j)}^2 + G_{(i,j)}^2 + B_{(i,j)}^2} < d_2 \wedge \sqrt{R_{(i,j)}^2 + G_{(i,j)}^2 + B_{(i,j)}^2} > d_3 \quad (2)$$

C. Feature Extraction

There exist some patterns that can differentiate bleeding region from non-bleeding region. In general, bleeding area shows dominant red, high saturation and low brightness. Naturally G and B are relatively low compared to R. Non-bleeding area has, on the other hand, low saturation, high brightness and bright color [6, 7]. However, the posture and location vary in the digestive tract all the time because the capsule operates inside the body and different LED intensity also affects the image quality. In the frame, the area closer to the capsule looks brighter and darker away from the capsule. For these reasons, we can have different values of color, saturation and brightness despite the same bleeding.

Considering these conditions, some features independent on brightness should be developed in order to diagnose bleeding. Fig. 3 shows the extinction coefficient of hemoglobin (Hb) and oxyhemoglobin (HbO_2) [8]. For blood, the ratios of the extinction coefficient in the bands of R (630-780 nm), G (490-560 nm) and B (450-490 nm) are rather independent on brightness. We chose the ratio of R with respect to G and B and the ratio of G and B as features. In addition, saturation was selected as another feature in the HSV color model since bleeding has a high value of saturation. The R band has lower extinction coefficient and reflects more light. Therefore, R values obtained through the image sensor become high. Normal tissue in digestive duct has very low value of R. R value is also selected as feature [9].

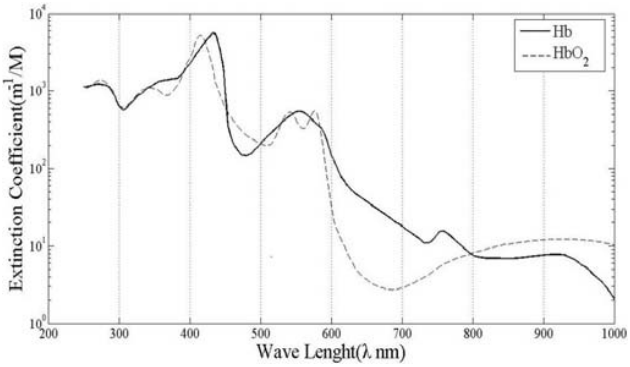

Fig. 3 The extinction coefficients of hemoglobin and oxyhemoglobin with respect to wavelength. Redrawn from data in [8]

In summary, the features are the ratio of R to G and B, the ratio between G and B, saturation in the HSV color model and normalized R values. They will be used as parameters in blood detection algorithm. The features in equations are given in the below.

$$F_1(i,j) = \frac{R_{(i,j)}}{\sqrt{G_{(i,j)}^2 + B_{(i,j)}^2}}$$

$$F_2(i,j) = \frac{G_{(i,j)}}{B_{(i,j)}}$$

$$F_3(i,j) = \frac{\max(R_{(i,j)}, G_{(i,j)}, B_{(i,j)}) - \min(R_{(i,j)}, G_{(i,j)}, B_{(i,j)})}{\max(R_{(i,j)}, G_{(i,j)}, B_{(i,j)})} \quad (3)$$

$$F_4(i,j) = R_{(i,j)} \ (Normalization)$$

D. Analysis and Classification

For a clearer distinction between bleeding and non-bleeding, we gave higher weight to bleeding region and lower weight to non-bleeding region based on the proposed features. In this way, was increased the distance between bleeding and non-bleeding in the normal distribution of the features. Therefore, they clearly show their characteristics and bleeding detection became easier.

1) Weight Calculation

Weighting factors that will enhance bleeding region are calculated by taking the optical properties and statistical analysis into account. Fig. 4 illustrates the normal distributions of the features on the bleeding sites from 30 images in the digestive tract. The rest six images with blood were not used in this calculation since their numbers of bleeding pixels were not sufficient enough to create a distribution profile statistically. As shown in Fig. 4, the mean value of $F_1(i,j)$ is about 2.3 and higher than any other features. If you look at Fig. 3, the contrast among RGB is clear. The extinction coefficient of B and G are high and that of R is small. Then, the actual color is inversely proportional to the extinction coefficient. Therefore, it explains that values of F_1 in Eq. (3) are larger. From the analysis of 30 images, we obtained high average values of $P_1(\mu_1 : 2.2914, \sigma_1 : 0.5026)$. In case of F_2, the ratio of G and B has $P_2(\mu_2 : 0.7345, \sigma_2 : 0.2316)$. Therefore, weighting factors, $W_1(i,j)$, $W_2(i,j)$ and $W_3(i,j)$ were assigned from their values of μ and σ and are given in Eq. (4).

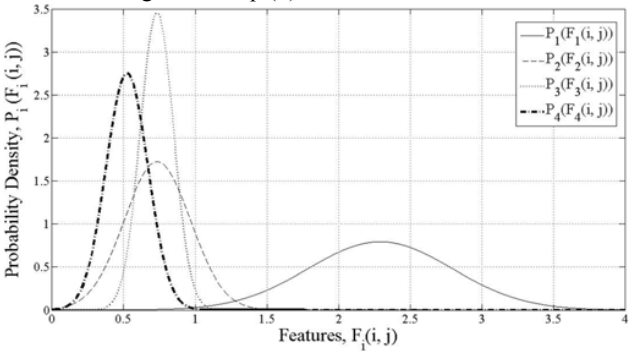

Fig. 4 The normal distribution of the features for bleeding pixels, $F_1(i,j)$ has $\mu_1 : 2.2914$, $\sigma_1 : 0.5026$, $F_2(i,j)$ has $\mu_2 : 0.7346$, $\sigma_2 : 0.2316$, $F_3(i,j)$ has $\mu_3 : 0.7325$, $\sigma_3 : 0.1155$, $F_4(i,j)$ has $\mu_4 : 0.5237$, $\sigma_4 : 0.145$

$$W_1(i,j) = \begin{cases} \alpha_1 e^{\frac{-[F_1(i,j)-\mu_1]}{2\sigma_1^2}} & , F_1(i,j) \le \mu_1 \\ \alpha_1 & , otherwise \end{cases}$$

$$W_2(i,j) = \begin{cases} \alpha_2 F_1(i,j) - \mu_2 & , F_2(i,j) \ge \mu_2 \\ 0 & , otherwise \end{cases}$$

$$W_3(i,j) = \begin{cases} \alpha_3 e^{\frac{-[F_3(i,j)-\mu_3]}{2\sigma_3^2}} & , F_3(i,j) \le \mu_3 \\ \alpha_3 & , otherwise \end{cases} \quad (4)$$

$$W_4(i,j) = \begin{cases} \frac{F_4(i,j)}{\mu_4} - \alpha_4 & , F_4(i,j) \ge \mu_4 \\ 0 & , otherwise \end{cases}$$

For P_1 and P_3 in case of bleeding, we did not attenuate the weighting factors since their values above the average distribution already indicate that the area had the features of blood. On the other hand, the weighting of F_4, $W_4(i,j)$, was assigned as attenuating factor when P_4 was lower than the average. $W_4(i,j)$ had an increasing weighting factor if P_4 was above the average. Finally, $W_T(i,j)$ for a certain wavelength in a particular frame (or image) was obtained by multiplying all the weighting factors. This is given by Eq. (5).

$$W_T(i,j) = W_1(i,j) \times W_2(i,j) \times W_3(i,j) \times W_4(i,j) \quad (5)$$

Pixel values were increased by $W_T(i,j)$ for the pixels that showed more characteristics of blood. Therefore, the distance between bleeding and non-bleeding was increased in the graphs of the normal distribution.

2) Classification

Once the distribution distance between bleeding and non-bleeding was clearly apart, we set thresholds and determined bleeding regions (Eq. 6). In our study, $T_1 = 1.5$ and $T_2 = 0.2$ were assigned.

$$\begin{cases} Bleeding & : F_1(i,j) \ge T_1 \wedge F_4(i,j) \ge T_2 \\ Non\text{-}Bleeding & : otherwise \end{cases} \quad (6)$$

E. Verification

In order to increase the accuracy of determining bleeding, an additional step was included. Once certain area in a frame was considered as bleeding site, it was compared with the neighboring blocks. Some patterns between the potential bleeding site and the neighboring blocks were examined. As shown in Fig. 5, the frame was divided into 20 x 20 blocks. The average values of some features were compared [10]. These features were $F_1(i,j)$, $F_3(i,j)$ and $F_4(i,j)$. $F_2(i,j)$ was not used since it did not affect the weighting factor substantially.

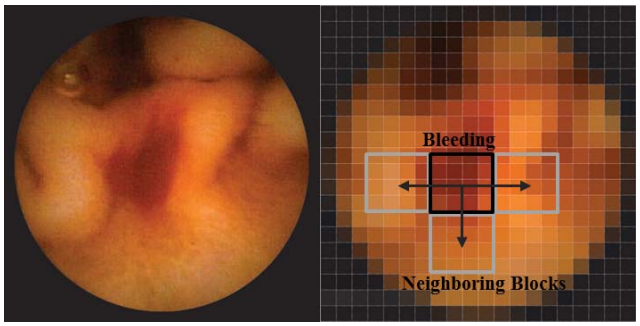

Fig. 5 The block-based verification; bleeding site was compared with the neighboring blocks as shown in the right figure in terms of their average values of the features

III. Experiment and Results

A. Experimental Environment

To verify our algorithms, we used a total of 42 images taken in the digestive tract. The majority of the images had bleeding in small vowel and more details are given in Table 1. The image data was processed using MATLAB v7.8 (The Mathworks Inc).

TABLE I
IMAGE SAMPLES

Diagnosis	The Number of the data
Small bowel bleeding	29
Angiodysplasia	2
Gastrointestinal Stromal tumor	1
Gastrorrhagia	2
Crohn's Disease	2
Normal	6
Total	42

B. Results

Fig. 6 shows the image at each step processed by the algorithms introduced in the previous sections. Fig. 6(a) is the original image with bleeding area in the center of the image frame. Fig. 6 (b) is the masked image which excluded the pixels not related with red. After this processing, the number of pixels to be computed was reduced substantially. Computation time was reduced accordingly. Weighting W_T based on the features was applied to Fig. 6 (b) and the result was Fig. 6 (c). Weighting increased the pixel values for the potential bleeding pixels. The pixel values of other region were reduced during weighting process. In this manner, the distance in the feature distribution between bleeding and non-bleeding regions was enhanced. Then, we determined as bleeding pixels if their values were higher than the threshold. Potential bleeding pixels shown in Fig. 6 (c) were gone through another step where bleeding block was compared with other neighboring blocks in terms of the feature values. The result was Fig. 6 (d).

Fig. 7 depicts the histogram of the feature distributions before and after weighting. Features F_2 and F_3 were not used in computing weighting factors. F_2 was not utilized in weighting since it is related only with green and blue. F_3 was also not used due to non-linearity characteristics among R, G and B colors.

Fig. 7 (a) is the histograms of $F_1(i,j)$ for bleeding and non-bleeding. Before weighting, the mean for bleeding was 1.766 and the mean for non-bleeding was 1.303. The difference was 0.463. As can be seen in Fig. 7 (a), two distributions before weighting were somewhat overlapped. The pixels in the overlapping region might be difficult to be diagnosed. Once weighting was applied the mean for bleeding became 3.401 with an increase of 1.634. The mean value of non-bleeding, on the other hand, decreased to 0.032 from 1.303. The distance between two distributions was 3.369. Recall that the distance before weighting was only 0.463.

Fig. 7 (b) is $F_4(i,j)$ histograms. Before weighting was applied, the mean value of pixels was 125.47 for bleeding and 71.11 for non-bleeding. After weighting, the mean value became 244.48 for bleeding and decreased to 1.91 in the case of non-bleeding. Weighting increased the distance from 54.36 to 242.57. It is easier to differentiate between bleeding and non-bleeding when the distance is bigger. Naturally, we can achieve higher prediction accuracy.

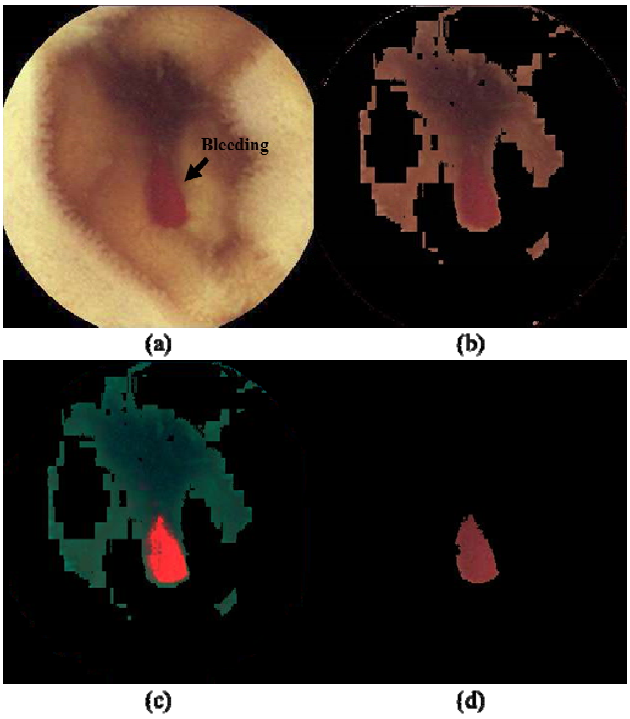

Fig. 6 The processed image at each step : (a) input image with a bleeding site in the center, (b) after Preprocessing, (c) after Analysis & Classification, (d) output image

Fig. 8 shows two other examples of bleeding detection. Fig. 8 (a) is a case with bleeding and Fig. 8 (c) is an image without bleeding. The results are Fig. 8 (b) and Fig. 8 (d) after our detection algorithm was applied. Fig. 8 (b) clearly detected bleeding areas. All black Fig. 8 (d) indicated that there was no bleeding in the image. The original images have 320x240 pixels.

We tested our method on 42 images of the digestive tract including bleeding and normal cases (Table I). The results are given in Table II. Bleeding or non-bleeding was checked for each pixel. The results were a sensitivity of 87% and a specificity of 90%. Sensitivity is defined as [true positive / (true positive + false negative)] and specificity, [true negative /(true negative + false positive)].

TABLE II
ACCURACY OF BLEEDING DETECTION FOR EACH PIXEL OUT OF 42 IMAGES

actual status	No. of pixels	predicted as bleeding	predicted as non-bleeding
bleeding	1,574,268	1,372,056	202,212
non-bleeding	1,742,400	182,255	1,560,145
total	3,316,668	1,554,311	1,762,357

IV. Conclusion

Our proposed method of detecting bleeding pixels was based on the parameters so called features in this study. Four features were chosen such that they can differentiate blood from normal tissue. Red-rated pixels were weighted to give more contrast on blood. Weighting was calculated based on the features. In addition, the potential blood pixels were compared to the neighboring pixels to be diagnosed as blood pixels.

Testing with 42 endoscope images, the prediction of bleeding or non-bleeding for a particular pixel had a sensitivity of 87% and a specificity of 90%. Computation involved in our method was not complex and easy enough to be implemented in capsule endoscopy.

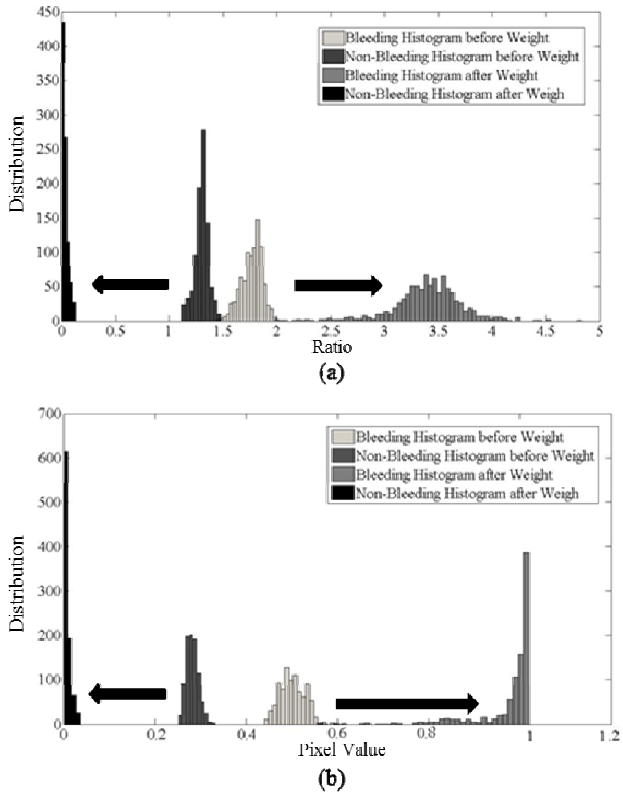

Fig. 7 Histograms of the features F_1 (a) and F_4 (b) before and after weighting was applied. Arrow direction indicates after weighting. After weighting, the distances between the mean values before and after weighting increased considerably

Acknowledgment

This work has been supported by Bilateral international cooperative research and development program, Ministry of Knowledge Economy, Republic of Korea.

We appreciate very much Professor J. Y. Park at Yonsei Medical School, Seoul, Korea for providing with the endoscope images.

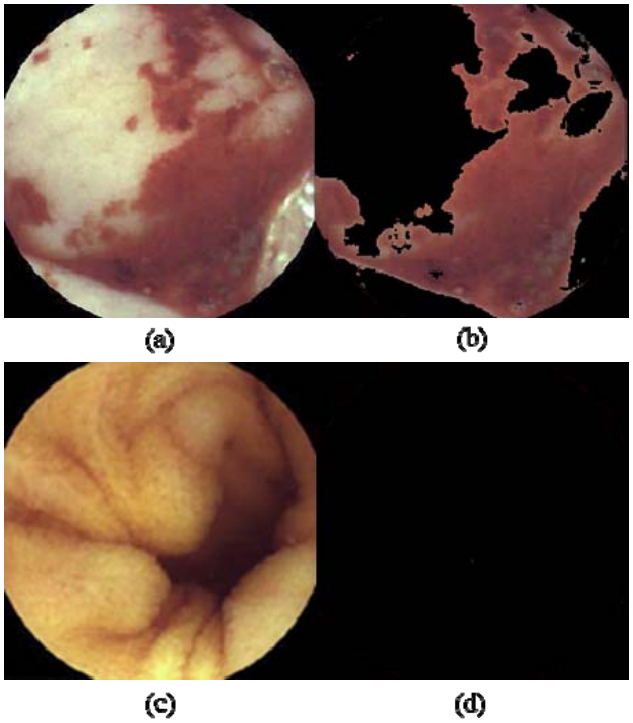

Fig. 8 Two examples of bleeding detection; (a) image with bleeding, (b) shows the predicted bleeding regions of (a) in red color, (c) image of normal tissue without any bleeding, (d) is after our detection algorithm was applied to (c) and all black in (d) shows that there was no bleeding. The image resolution was 320x240 pixels

References

[1] N. Bourbakis, "Detecting abnormal patterns in WCE images" in *5th IEEE Symp. on Bioinformatics and Bioengineering (BIBE'05)*, 2005, pp. 232–328.

[2] Intromedic Corp., South Korea, www.intromedic.com.

[3] A. Glukhovsky, "Wireless capsule endoscopy", *Sensor Review*, vol. 23, no. 2, 2003, pp. 128–133.

[4] L. Cui, C. Hu, Y. Zou, and M. Q.-H. Meng, "Bleeding Detection in Wireless Capsule Endoscopy Images by Support Vector Classifier" in *2010 IEEE Int. Conf. on Information and Automation (ICIA)*, 2010, pp. 1746-1751.

[5] A. Karahyris, and N. Bourbakis, "A Methodology for Detecting Blood-based Abnormalities in Wireless Capsule Endoscopy Videos" in 8th *IEEE Int. Conf. on Bioinformatics and Bio Engineering (BIBE'08), 2008*, pp. 1-6.

[6] G. Pan, G. Yan, X. Qui, and J. Cui, "Bleeding Detection in Wireless Capsule Endoscopy Based on Probabilistic Neural Network" *Journal of Medical Systems*, vol. 34, Jan. 2010.

[7] P. Y. Lau, and P. L. Correia, "Detection of Bleeding patterns in WCE video using multiple features" *29th Annual Int. Conf. of the IEEE Engineering in Medicine and Biology Society, 2007, pp. 5601-5604.*

[8] S. A. Prahl., Tabulated molar extinction coefficient for hemoglobin in water. Oregon Medical Laser Center 2001. Available at: http://omlc.ogi.edu/spectra/hemoglobin/. Accessed May 13, 2004.

[9] P. Y. Lau, and P. L. Correia, "Analyzing Gastrointestinal Tissue Images using Multiple Features" in *6th Conf. on Telecommunications*, Peniche, 2007, pp. 435-438.

[10] C. K. Poh, T. M. Htwe, L. Li, W. Shen, j. Liu, J. H. Lim, K. L. Chan, and P. C. Tan, "Multi-Level Local Feature Classification for Bleeding Detection in Wireless Capsule Endoscopy images" in 2010 *IEEE conf. on Cybernetics and Intelligent Systems, 2010, Singapore, pp. 76-81.*

Yong-Gyu Lee was born in Seong-nam, South Korea (1984) and received his B.S. degree in electronics and information engineering from Seoul National University of Science and Technology, Seoul, South Korea (2010). He is currently a M.S. student at Seoul National University of Science and Technology and engages in biomedical engineering.

Gilwon Yoon received his B.S. in Electrical Engineering from Seoul National University, Seoul, Korea in 1977 and M.S. and Ph.D. in Electrical and Computer Engineering from the University of Texas at Austin, U.S.A. in 1982 and 1988 respectively. From 1990 to 1992, he was a research engineer at Dixon Utah Laser Institute, Salt Lake City, USA. He worked at Samsung Advanced Institute of Technology, Korea between 1992 and 2003. He is with Seoul National University of Science and Technology since 2003.